腫瘍集積トランスポーターとしてヒトグリオブラストーマ細胞株を標的とする新規細胞膜透過性ペプチドの同定

Identification of a novel cell-penetrating peptide targeting human glioblastoma cell lines as a cancer-homing transporter

Moritoshi Higa[1], Chiaki Katagiri[2], Shimizu-Okabe C[3], Tomoyuki Tsumuraya[1], Masanori Sunagawa[1], Mariko Nakamura[1], Shogo Ishiuchi[2], Chitoshi Takayama[3], Eisaku Kondo[4]and Masayuki Matsushita[1]

[1]Department of Molecular and Cellular Physiology
[2]Department of Neurosurgery
[3]Department of Molecular Anatomy
Graduate School of Medicine, University of the Ryukyus, 903-0215 Okinawa, Japan
[4]Division of Oncological Pathology
Aichi Cancer Center Research Institute, Nagoya, Japan

Running title: Glioblastoma homing cell-penetrating peptide
Keywords: CPP, glioblastoma, p16, imaging, DDS

Correspondence should be addressed to
Masayuki Matsushita
Department of Molecular and Cellular Physiology
Graduate School of Medicine
University of the Ryukyus, Okinawa 903-0215, Japan
Tel: +81-98-895-1106; Fax: +81-98-895-1402
E-mail: masayuki@med.u-ryukyu.ac.jp

The authors disclose no potential conflicts of interest.

ABSTRACT

Cell-penetrating peptides (CPPs) as a novel biomedical delivery system have been highly anticipated, since they can translocate across biological membranes and are capable of transporting their cargo inside live cells with minimal invasiveness. However, non-selective internalization in various cell types remains a challenge in the clinical application of CPPs, especially in cancer treatment. In this study, we attempted to identify novel cancer-homing CPPs to target glioblastoma multiforme (GBM), which is often refractory and resistant to treatment. We screened for CPPs showing affinity for the human GBM cell line, U87MG, from an mRNA display random peptide library. One of the candidate peptides which amino-acid sequence was obtained from the screening showed selective cell-penetrating activity in U87MG cells. Conjugation of the $p16^{INK4a}$ functional peptide to the GBM-selective CPP induced cellular apoptosis and reduced phosphorylated retinoblastoma protein levels. This indicates that the CPP was capable of delivering a therapeutic agent into U87MG cells inducing apoptosis. These results suggest that the novel CPP identified in this study permeates with high affinity into GBM cells, revealing it to be a promising imaging and therapeutic tool in the treatment of glioblastoma.

1. INTRODUCTION

Glioblastoma multiforme (GBM, WHO grade IV astrocytoma) is the most common malignant brain tumor originating in the central nervous system in adults. Despite advances in surgical resection, chemotherapy, and radiotherapy combined with adjuvant therapy, the median survival in patients with GBM is generally less than 12 months after the time of diagnosis because of its rapid progression and invasive nature[1]. Thus, there is an urgent need for more effective therapeutic strategies for refractory GBM.

Recently, cell-penetrating peptides (CPPs), also referred to as protein transduction domains (PTDs), which have the ability to permeate across the plasma membrane and can facilitate the efficient cellular internalization of biomolecules, have attracted attention as peptide-based delivery systems [2,3]. To date, CPPs such as the human immunodeficiency virus type1 (HIV-1) transcriptional activator TAT protein [4], the Antenapedia (Antp) homeodomain of *Drosophila* [5], and poly-arginine ((Arg)n, n = 4-16) [6,7] have been the most widely studied with respect to enhancing the intracellular delivery of CPP-conjugated molecules. Since these peptides could efficiently deliver a variety of biological macromolecules, including proteins, peptides, DNAs, RNAs and nanoparticles into various living cells with minimal cytotoxicity, the use of CPPs as a delivery system to directly introduce biologically active molecules into cells has been

expected [2,8,9]. However, from a clinical point of view, non-selective internalization of CPPs into various cells is the limiting factor for cell-type or tissue specific targeting applications such as cancer treatments [4,10]. Development of target-selective CPPs may contribute to improving therapeutic efficacy and reducing side effects on normal tissues [11,12]. Accordingly, the purpose of the present study was to identify novel CPPs targeting GBM as selective transporters.

mRNA displayed peptides comprise a genotype (mRNA/cDNA) template and phenotype (nascent protein) that is encoded by its mRNA, and are linked by a covalent bond through the puromycin linker [13]. The *in vitro* cell-free protein synthesis system boasts a diversity of approximately 10^{12}-10^{13} individual sequences, each containing 10 contiguous random amino acids that are encoded by a synthetic cDNA library (templates), which is greater than that of phage display technology ($<10^{9}$) [14]. The amino acid sequence of an mRNA displayed polypeptide can be identified easily by nucleic acid sequencing [15,16]. Thus, mRNA display technology provides a means of screening for useful physiologically active peptides and novel functional proteins. Here, we aimed to investigate novel CPPs with an affinity for the U87MG human GBM cell line using an mRNA display random peptide library *in vitro*. In this article, we present a novel CPP as a potential tool for GBM selective intracellular delivery.

2. MATERIALS & METHODS

2.1. Peptide synthesis

All peptides in the present study were synthesized chemically by SIGMA-ALDRICH (Tokyo Japan). Peptide purity was 90% or greater, which was confirmed by high-performance liquid chromatography analysis and mass spectroscopy. Peptides were dissolved in distilled water to generate 1 mM stock solutions.

2.2. Cell culture

The human glioblastoma (GBM) cell line U87MG used in the present study was purchased from the American Type Culture Collection (USA). The other cell lines used for *in vitro* assays are shown in Table 1. All human cell lines were maintained in Dulbecco's modified Eagle's medium (DMEM) (Invitrogen) supplemented with 10% (v/v) heat-inactivated fetal bovine serum (FBS) (Invitrogen), 100 U/ml penicillin, and 100 μg/ml streptomycin (Invitrogen) at 37^{o}C with 5% CO_2. Primary cultured neurons were obtained from the hippocampus of 18-embryonic-day fetal C57BL6/J mice and maintained in neurobasal medium supplemented with 2% B-27 (Invitrogen), 1% penicillin/streptomycin, and 0.5 mM L-glutamine.

2.3. Fluorescence cellular imaging and quantitative analysis

Cells were seeded at a density of 3×10^5 cells per 35 mm glass bottom dish and incubated with 10 μM of FITC-labeled peptides in complete medium for 2 h at 37^{o}C. For fluorescence microscopy imaging, cells were washed twice with fresh medium, and cell fluorescence was immediately analyzed using confocal laser scanning microscopy (CLSM) (Olympus Tokyo Japan, FLUOVIEW FV-1000) without fixation. Fluorescence intensities at the region of interest (ROI) of 3 cells per microscopic image were measured by Meta Morph software Version 6 (Olympus), and experiments were conducted in triplicate. Background fluorescence intensity was subtracted from all experiments. For fluorescence-activated cells sorting (FACS) analysis, the cells were washed twice with phosphate-buffered saline (PBS) and collected by trypsinization. Detached cells were resuspended in FACS buffer (PBS, 2% FBS), then samples (1×10^4 cells) were immediately subjected to flow cytometric analysis (MILLIPORE Guava Easy Cyte Plus) using guava soft version2 (MILLIPORE) without fixation.

2.4. RT-PCR

Total RNA was extracted with TRIzol (Invitrogen) from the human glioblastoma cell

lines U87MG and U118MG, and HeLa cells. cDNA was synthesized from the RNA product using an oligo (dT) primer and cDNA synthesis kit (TAKARA) according to the manufacturer's instructions. Reverse transcription-PCR was performed with Ex-Taq polymerase (TAKARA) under the following amplification conditions: denaturation at 94 ^{o}C for 2 min, followed by 40 cycles of denaturation at 98 ^{o}C for 10-s, annealing at 55 ^{o}C for 30-s, extension at 72 ^{o}C for 2 min, and a final extension at 72 ^{o}C for 10 min. The sense/antisense primer sequences for human $p16^{INK4a}$ were 5'-TTCCTGGACACGCTGGTGGTG-3' and 5'-GGCATCTAT GCGGGCATGGTTA-3', respectively. Actin was used as internal standard gene.

2.5. Detection of apoptotic cells

U87MG cells were seeded at a density of 5×10^5 cells per 60 mm dish and incubated with 20 μM of peptide1NSΔ-p16 MIS or peptide1NSΔ-p16 V95E in complete medium for 4 h at 37 ^{o}C, respectively. After treatment, the cells were washed twice with PBS and collected by trypsinization. Then, the cells were resuspended in 100 μl of binding buffer (0.5 M HEPES pH 7.4, 1 M NaCl, 1M KCl, 1M $MgCl_2$, 0.2 M $CaCl_2$) containing 5 μl FITC-Annexin V (BD Pharmingen) and 5 μl Propidium iodide (PI) (SIGMA-ALDRICH), and incubated under darkness for 15 min according to the

manufacturer's instructions. The cells were immediately subjected to flow cytometric analysis at 1×10^4 cells per sample.

2.6. Western blotting

U87MG cells were seeded at a density of 3×10^5 cells to 35mm well plate and incubated with 20 μM of peptide1NSΔ-p16 MIS or peptide1NSΔ-p16 V95E in DMEM under a serum free condition for 24 h at 37 ^{o}C, respectively. After treatment, the cells were washed with complete medium and further incubated at 37 ^{o}C for 4 h. Then, the cells were lysed with 2×SDS sample buffer, and extracts were separated by sodium dodecyl sulphate polyacrylamide gel electrophoresis (SDS-PAGE) using an 8% SDS-PAGE gel and transferred onto a nitrocellulose membrane (BIO-RAD). After blocking with Blocking One (NACALAI TESQUE), the membrane was sequentially probed with the following antibodies: primary antibodies were rabbit polyclonal anti-Ser 807/811 phosphorylated pRB antibody 1:1000 (CST, Cell Signaling Technology), and anti-actin monoclonal antibody 1:3000 (Chemicon); secondary antibodies were anti-rabbit antibody 1:3000 (CST), and anti-mouse antibody 1:3000 (Millipore). After washing with Tris-buffered saline Tween solution (TBS-T), signals were detected using ECL Prime Western Blotting Detection Reagent (GE Healthcare) and Versa Doc (BIO-RAD).

Quantifications were carried out by densitometric analysis using Quantity One software (BIO-RAD).

2.7. Statistical analysis

Statistical significance was calculated using Statcel 3 software (OMS publishing Inc.). A student's *t*-test was used for data analysis and p value < 0.05 was considered statistically significant. All values are shown as means ± standard deviation (SD) from at least 3 independent experiments.

3. RESULTS

3.1. Screening for candidate CPPs targeting U87MG GBM cells.

First, to identify peptides capable of permeating into glioblastoma multiforme (GBM), we screened for cell-penetrating peptides (CPPs) targeting the human GBM cell line U87MG from an mRNA displayed random peptide library (Fig. 1A). The mRNA display library was constructed as previously described [13]. From about 60 sequences derived from concentration libraries, we randomly selected ten candidates and synthesized chemically fluorescein isothiocyanate (FITC)-labeled peptides (Fig. 1B). Nona-arginine (RRRRRRRRR: R9) was used as a nonselective permeation CPP. To

evaluate the cell-penetrating activity of these peptides, U87MG cells were incubated with 10 μM of each numbered FITC-labeled peptide. We examined intracellular fluorescence signals in cells using confocal laser scanning microscopy (CLSM) (Fig. 1C). Moreover, we confirmed their mean fluorescence intensity using Meta Morph software (Fig. 1D). Consequently, we identified a novel CPP, peptide1 (NTCTWLKYHS), whose cell-penetrating activity was stronger than the other candidates.

3.2. Peptide1 is incorporated selectively into GBM cells.

Because peptide1 showed the best cell-penetrating activity into U87MG cells, we further investigated its GBM cell selectivity using cells derived from various tissues (Table 1). Fluorescent images and quantitative analysis showed high selective permeability of the peptide1 into U87MG cells compared with other cell lines (Fig. 2A, B). As shown in Fig. 2C, FITC-labeled peptide1 also permeated into the U118MG GBM cell line. These results indicate that peptide1 might have selective permeability into GBM cells.

3.3. Peptide1-NSΔ exhibits increased cell-penetrating activity in U87MG cells.

To improve penetration efficiency, we modified the amino acid sequence of peptide1. In one sequence, Cys (C) was substituted with Gly (G), because Cys might allow disulfide bonding to other proteins; in the other sequences, N- and/or C- terminus amino acid residues were deleted in each mutant peptide (Table 2). We synthesized seven FITC-labeled peptide1 variants, and examined intracellular fluorescence signals in U87MG cells using CLSM and flow cytometry. Images showed that the fluorescence signals of peptide1-NSΔ (TCTWLKYH) and peptide1-NTSΔ (CTWLKYH) increased compared with peptide1, although they were inferior to R9 as a positive control (Fig. 3A). Fluorescence-activated cell sorting (FACS) analysis revealed that intracellular localization of the FITC-labeled peptide1-NSΔ was 2.0-fold higher than that of peptide1 (Fig. 3B). On the other hand, C3G (NTGTWLKYHS), NTCSΔ (TWLKYH), and NTHSΔ (CTWLKY) were decreased. Further, fluorescence images and quantitative analysis showed that peptide1-NSΔ preserves the permeability into U87MG and U118MG cell lines (Fig. 3C, D). These results suggest that peptide1-NSΔ has potential as a GBM homing intracellular transporter.

3.4. Antitumor effect of p16 MIS fusion peptide1-NSΔ against U87MG cells.

Deficiency of the $p16^{INK4a}$ tumor suppressor gene is frequently found in the majority of

human cancers including GBM [17]. Expression loss of the $p16^{INK4a}$ gene in both U87MG and U118MG cell lines was confirmed by reverse transcription-PCR (Fig. 4A). Therefore, to assess whether peptide1-NSΔ can deliver cargo into U87MG cells, we focused on a small peptide that comprises the minimal inhibitory sequence of p16 (FLDTLVVLHR: p16 MIS), the function of which was described in previous studies [18,19]. The antitumor peptide was designed by fusing peptide1-NSΔ and p16 MIS (peptide1NSΔ-p16 MIS) via the Gly-Pro-Gly spacer, and R4 (RRRR) was tagged at its C-terminus to enhance solubility. Peptide1NSΔ-p16 V95E, which substitutes valine 95 (V95) in the MIS sequence with glutamate (E), was used as a control (Fig. 4B). U87MG cells were treated with 20 μM of peptide1NSΔ-p16 MIS or peptide1NSΔ-p16 V95E for 4 h. After treatment, FACS analysis using Annexin V-FITC and PI (propidium iodide) showed that the early apoptosis rate increased significantly in the p16 MIS conjugate-treated cells (70 ± 6.25 %) compared with p16 V95E conjugate-treated cells (10 ± 3.26%) and untreated cells (12 ± 1.70%) (Fig. 4C, *right graph*). Furthermore, to confirm whether cellular apoptosis was caused by the p16 MIS, we examined the phosphorylation status of retinoblastoma protein (pRB), which is regulated by Cdk4/6, the target for $p16^{INK4a}$. Twenty-four hours after treatment, western blot analysis revealed that phosphorylated pRB (p-pRB) ($Ser^{807/811}$ phosphorylation) was significantly

decreased only in the p16 MIS-treated cells compared with the p16 V95E-treated cells. The p-pRB levels of untreated cells and p16 V95E-treated cells were the same in U87MG cells (Fig. 4D, E). The levels of phosphorylated pRB correlate with the induction of early apoptosis shown in Figure. 4C. These results demonstrated that peptide1-NSΔ can deliver the p16 functional peptide into U87MG cells as a transporter.

4. DISUCUSSION

Targeted cancer therapy holds promise by reducing adverse effects on normal cells and enhancing therapeutic effects [20]. Because CPPs have high biocompatibility and can deliver efficiently a variety of biologically active cargos into cells, studies of cancer-specific drug delivery systems using CPPs have been widely carried out.

In the present study, we report on the GBM selective CPP, peptide1-NSΔ (TCTWLKYH), which was obtained using mRNA display technology. A protein database search revealed that this peptide appears to encode an artificial sequence, as it has no significant identity to any recorded mammalian proteins, including previously reported CPP sequences. The fluorescence-labeled peptide1-NSΔ was incorporated selectively into U87MG GBM cells *in vitro* (Fig. 3C,D). In most human malignancies, genetic abnormality of tumor suppressor genes has been well characterized [21]. In

particular, expressional loss of $p16^{INK4a}$ occurs in U87MG cells (Fig. 4A) [22,23]. The $p16^{INK4a}$ tumor-suppressor gene has been found to be homozygously deleted, mutated or transcriptionally inhibited by methylation in GBMs [24]. $p16^{INK4a}$ binds directly to and inhibits the activity of CDK4 and CDK6, the D-type cyclin-dependent kinases that initiate the phosphorylation of pRB [25], leading to cellular apoptosis and senescence as a result of G1/S phase cell cycle arrest [26]. Analysis of a variety of human cancers has revealed a pattern in the pathway, in which only one of the four members such as cyclin D1, CDK4/CDK6, p16, and pRB of the $p16^{INK4a}$/CDK/pRB pathway is inactivated [27]. Therefore, restoration of the p16INK4a/CDK/pRB pathway is proposed to be an attractive target for therapeutic intervention because of its important role in cancer development as a cell cycle-regulatory pathway. The peptide1-NSΔ conjugated p16 MIS functional peptide induced a decrease in the level of phosphorylated pRB and an increase in early cellular apoptosis (Fig. 4C,D). These results suggest that peptide1-NSΔ can deliver imaging and antitumor agents into U87MG cells as a transporter.

In previous studies, CPPs such as HIV1-TAT and poly-arginine were used as intracellular delivery vehicles in a variety of cell types including peripheral blood lymphocytes, diploid human fibroblasts, keratinocytes, bone marrow stem cells, osteoclasts, fibrosarcoma cells, osteosarcoma, glioma, hepatocellular carcinoma, renal

carcinoma, and NIH 3T3 cells (mouse fibroblast-like cell line)[4]. The most important observation in this study is that peptide1-NSΔ was incorporated selectively into GBM cell lines as compared with other cell lines (Fig. 3C). Although the mechanism responsible for the selective penetration of peptide1-NSΔ into GBM remains unclear, this unique ability differs notably from the existing CPPs mentioned previously, which enables the targeting function as a GBM-homing peptide.

This study has several limitations. Fluorescence signals of peptide1-NSΔ were detected at low levels in several cell lines, especially HepG2 and HeLa cells (Fig. 3D). Therefore, these findings may indicate that the level of selectivity requires further improvement in order to warrant designation as a GBM-specific delivery system. Moreover, when we added p16 MIS conjugates to the cell culture medium, aggregates in the medium were observed (data not shown), probably due to the interaction of proteins contained in the medium with the conjugates. This observation indicates that the functionality of this system is likely to be limited by solubility issues. Also, it seems likely that various environmental factors, including concentration, treatment time, medium components, and cell sensitivity, are involved in an optimum effect. Thus, further improvement of both the solubility and stability of the p16 MIS conjugate in the medium is needed. .

In conclusion, we identified a novel CPP, peptide1-NSΔ, which exhibits selectivity to the U87MG GBM cell line and is capable of delivering its payload into cells *in vitro*. Our findings may provide new avenues for both effective therapeutics and diagnostics in clinical applications as a peptide based delivery system. However, the critical mechanism of tumor selectivity remains to be elucidated. Consequently, further research is required to clarify the GBM-selective recognition mechanisms.

ACKNOWLEDEMENTS

This research was supported by grants-in-aid for scientific research from the Japanese Ministry of Education, Culture, Sports, Science and Technology (MEXT) (M.M.). This research was also supported by the Uehara Memorial Foundation, Takeda Science Foundation, Special Account Budget for Education and Research granted from MEXT and The Promotion Project of Medical Clustering of Okinawa prefecture (M.M.).

REFERENCES

[1] R. Stupp, W.P. Mason, M.J. van den Bent, M. Weller, B. Fisher, M.J.B. Taphoorn, et al., Radiotherapy plus concomitant and adjuvant temozolomide for glioblastoma., N. Engl. J. Med. 352 (2005) 987–96. doi:10.1056/NEJMoa043330.

[2] J.S. Wadia, S.F. Dowdy, Protein transduction technology., Curr. Opin. Biotechnol. 13 (2002) 52–6.

[3] M.C. Morris, J. Depollier, J. Mery, F. Heitz, G. Divita, A peptide carrier for the delivery of biologically active proteins into mammalian cells., Nat. Biotechnol. 19 (2001) 1173–6. doi:10.1038/nbt1201-1173.

[4] S.A.E.& S.F.D. Hikaru Nagahara, Adamina M. Vocero-Akbani, Eric L. Snyder, Alan Ho, Dawn G. Latham, Natalie A. Lissy, Michelle Becker-Hapak, Transduction of full-length TAT fusion proteins into mammalian cells : TAT-p27 Kip1 induces cell migration, Nat. Med. (1998) 1449−1452.

[5] D. Derossi, a H. Joliot, G. Chassaing, a Prochiantz, The third helix of the Antennapedia homeodomain translocates through biological membranes., J. Biol. Chem. 269 (1994) 10444–50.

[6] S. Futaki, T. Suzuki, W. Ohashi, T. Yagami, S. Tanaka, K. Ueda, et al., Arginine-rich Peptides, J. Biol. Chem. 276 (2001) 5836–5840. doi:10.1074/jbc.M007540200.

[7] E. Kondo, M. Seto, K. Yoshikawa, Highly efficient delivery of p16 antitumor peptide into aggressive leukemia / lymphoma cells using a novel transporter system, Mol. Cancer Ther. (2005) 1623–1630.

[8] H. Noguchi, S. Matsumoto, Protein transduction technology: a novel therapeutic perspective., Acta Med. Okayama. 60 (2006) 1–11.

[9] E.K. and V.P.T. Torchilin, Cell-penetrating peptides: breaking through to the other side, Trends Mol. Med. 18 (2012) 385–393.

[10] S.F.D. Jehangir S. Wadia, Transmembrane delivery of protein and peptide drugs by TAT-mediated transduction in the treatment of cancer, Adv. Drug Deliv. Rev. (2005) 579–596.

[11] K.J. Lim, B.H. Sung, J.R. Shin, Y.W. Lee, D.J. Kim, K.S. Yang, et al., A Cancer Specific Cell-Penetrating Peptide, BR2, for the Efficient Delivery of an scFv into Cancer Cells., PLoS One. 8 (2013) e66084. doi:10.1371/journal.pone.0066084.

[12] E. Kondo, K. Saito, Y. Tashiro, K. Kamide, S. Uno, T. Furuya, et al., Tumour lineage-homing cell-penetrating peptides for peptide-based anti-cancer molecular delivery systems, Nat. Commun. 951 (2012) 1–13.

[13] K. Kamide, H. Nakakubo, S. Uno, A. Fukamizu, Isolation of novel cell-penetrating peptides from a random peptide library using in vitro virus and their modifications, Int. J. Mol. Med. 25 (2010) 41–51. doi:10.3892/ijmm.

[14] D. Lipovsek, A. Plu, In-vitro protein evolution by ribosome display and mRNA display, J. Immunol. Methods. 290 (2004) 51–67. doi:10.1016/j.jim.2004.04.008.

[15] N. Nemoto, E. Miyamoto-Sato, Y. Husimi, H. Yanagawa, In vitro virus: bonding of mRNA bearing puromycin at the 3'-terminal end to the C-terminal end of its encoded protein on the ribosome in vitro., FEBS Lett. 414 (1997) 405–8.

[16] E. Miyamoto-Sato, M. Ishizaka, K. Horisawa, S. Tateyama, H. Takashima, S. Fuse, et al., Cell-free cotranslation and selection using in vitro virus for high-throughput analysis of protein-protein interactions and complexes., Genome Res. 15 (2005) 710–7. doi:10.1101/gr.3510505.

[17] H. Ohgaki, P. Kleihues, Genetic pathways to primary and secondary glioblastoma., Am. J. Pathol. 170 (2007) 1445–53. doi:10.2353/ajpath.2007.070011.

[18] K.L.B. and D.P.L. Robin Fahraeus, Sonia Lain, Characterization of the cyclin-dependent kinase inhibitory domain of the INK4 family as a model for a synthetic tumour suppressor molecule, Oncogene. 16 (1998) 587–596.

[19] E. Kondo, T. Tanaka, T. Miyake, T. Ichikawa, M. Hirai, M. Adachi, et al., Potent synergy of dual antitumor peptides for growth suppression of human

glioblastoma cell lines., Mol. Cancer Ther. 7 (2008) 1461–71. doi:10.1158/1535-7163.MCT-07-2010.

[20] L. Agemy, D. Friedmann-Morvinski, V.R. Kotamraju, L. Roth, K.N. Sugahara, O.M. Girard, et al., Targeted nanoparticle enhanced proapoptotic peptide as potential therapy for glioblastoma., Proc. Natl. Acad. Sci. U. S. A. 108 (2011) 17450–5. doi:10.1073/pnas.1114518108.

[21] M. Weller, J. Rieger, C. Grimmel, E.G. Van Meir, N. De Tribolet, S. Krajewski, et al., Predicting chemoresistance in human malignant glioma cells: the role of molecular genetic analyses., Int. J. Cancer. 79 (1998) 640–4.

[22] J. He, J.J. Olson, C.D. James, C. Lines, Lack of p16 INK4 or Retinoblastoma Protein (pRb), or Amplification-associated Overexpression of cdk4 Is Observed in Distinct Subsets of Malignant Glial Tumors and Cell Lines, Cancer Res. 55 (1995) 4833–4836.

[23] F.D. Ragione, G.L. Russo, a. Oliva, C. Mercurio, S. Mastropietro, V.D. Pietra, et al., Biochemical Characterization of p16INK4- and p18-containing Complexes in Human Cell Lines, J. Biol. Chem. 271 (1996) 15942–15949. doi:10.1074/jbc.271.27.15942.

[24] M. a Al-Mohanna, P.S. Manogaran, Z. Al-Mukhalafi, K. A Al-Hussein, A. Aboussekhra, The tumor suppressor p16(INK4a) gene is a regulator of apoptosis induced by ultraviolet light and cisplatin., Oncogene. 23 (2004) 201–12. doi:10.1038/sj.onc.1206927.

[25] J. Calbó, M. Marotta, M. Cascalló, J.M. Roig, J.L. Gelpí, J. Fueyo, et al., Adenovirus-mediated wt-p16 reintroduction induces cell cycle arrest or apoptosis in pancreatic cancer., Cancer Gene Ther. 8 (2001) 740–50. doi:10.1038/sj.cgt.7700374.

[26] K. Zennami, K. Yoshikawa, E. Kondo, K. Nakamura, Y. Upsilonamada, M. a De Velasco, et al., A new molecular targeted therapeutic approach for renal cell carcinoma with a p16 functional peptide using a novel transporter system., Oncol. Rep. 26 (2011) 327–33. doi:10.3892/or.2011.1290.

[27] K. Fujimoto, R. Hosotani, Y. Miyamoto, R. Doi, T. Koshiba, a Otaka, et al., Inhibition of pRb phosphorylation and cell cycle progression by an antennapedia-p16(INK4A) fusion peptide in pancreatic cancer cells., Cancer Lett. 159 (2000) 151–8.

FIGURE LEGENDS

Table 1. Cell lines of histologically different origins, including human GBM, were used in the cell-penetration assay. Primary cultured mouse neurons were used as a non-neoplastic counterpart.

Figure 1. Screening of candidate CPPs with an affinity for U87MG cells.

(A) Scheme of screening for CPPs using mRNA display technology. (1) Construction of mRNA display random peptide libraries in a cell-free translation system. (2) Peptide libraries in the solution were added to the U87MG cell medium. (3) Extracellular peptides were removed by trypsinization and washing. (4) The genomes of chimeric molecules incorporated into the cells were recovered and amplified by their anchored template cDNA using PCR. (5) Reconstruction of mRNA display random peptide libraries for the next selection cycles. (6) After the selection cycles, the peptide sequences of candidate CPPs were predicted by cloning and sequencing. (B) List of peptide sequences selected randomly from the peptides obtained by screening. Poly-arginine (R9) was used as a representative nonselective permeable CPP. (C) U87MG cells were treated with 10 μM of each numbered FITC-labeled peptide for 2 h

at 37°C. Fluorescence images were observed using CLSM. Scale bar, 200 μm. (D) Meta Morph quantitative analysis of fluorescence intensity of ten candidate CPPs in U87MG cells. The mean fluorescence intensity of the peptides against background was calculated in each image obtained by fluorescence microscopy. a.u.; arbitrary unit. Data are presented as the means ± SD of 3 independent experiments.

Figure 2. Cell-penetration assay of peptide1 using cells derived from various tissues.

(A) Histologically different cell types were treated with 10 μM of FITC-labeled peptide1 for 2 h at 37°C. Fluorescence images were observed using CLSM. Scale bar, 50 μm. (B) Meta Morph quantitative analysis of fluorescence intensity of peptide1 in cells. The mean fluorescence intensity of peptide1 against background was calculated in each image obtained by fluorescence microscopy. a.u.; arbitrary unit. Data are presented as the means ± SD of 3 independent experiments. (C) Fluorescence images of FITC-labeled peptide1 in U118MG. These cells were treated under the same conditions as mentioned above.

Table 2. Peptide1-C3G was substituted Cys (C) with Gly (G), and peptide1 deletion series were made by deleting residues from N- and/or C- terminus.

Figure 3. Analysis of the cell-penetration efficiency of peptide1 variants.

(A) U87MG cells were treated with 10 μM of FITC-labeled peptide1 variants for 2 h at 37^{o}C. Fluorescence images were observed using CLSM. Scale bar, 200 μm. (B) FACS quantitative analysis of mean fluorescence intensity of the peptide1 variants in U87MG cells. The relative fluorescence intensity of each peptide compared with peptide1 (1.0) was measured using flow cytometry. Data are presented as means ± SD of 3 independent experiments. (C) Histologically different cell types were treated with 10 μM of FITC-labeled peptide1-NSΔ for 2 h at 37^{o}C. Fluorescence images were observed using CLSM. Scale bar, 50 μm. (D) Meta Morph quantitative analysis of fluorescence intensity of peptide1-NSΔ in cells. The mean fluorescence intensity of peptide1-NSΔ against background was calculated in each image obtained by fluorescence microscopy. a.u.; arbitrary unit. Data are presented as means ± SD of 3 independent experiments.

Figure 4. Therapeutic effect of peptide1NSΔ-p16 MIS conjugates against U87MG cells.

(A) RT-PCR analysis of the endogenous mRNA expression of the p16^{INK4a} tumor suppressor gene in two human GBM cells, U87MG and U118MG. HeLa cells were used as a positive control. (B) Design of CPP-p16 antitumor peptide conjugate, which is

composed of peptide1-NSΔ and the functional amino acid sequence of $p16^{INK4a}$ (p16 MIS: minimal inhibitory sequence). p16 V95E was used as a control that substitutes valine 95 (V95) in the MIS sequence with glutamate (E). (C) FACS analysis for cellular apoptosis in U87MG cells treated with 20 μM of peptide1-NSΔ fused with p16 MIS or p16 V95E for 4 h, respectively. Cells in the lower right quadrant (Annexin V positive / PI negative) represent early apoptotic cells. Percentage of early apoptotic cells (*right*). Data are presented as the means ± SD of 3 independent experiments per treatment group. (D) Phospho-$Ser^{807/811}$ pRB (p-pRB) status in U87MG cells was assessed by western blotting. Cells were treated with 20 μM of peptide1-NSΔ fused with p16 MIS or p16 V95E for 24 h, respectively. (E). Ratio of p-pRB/actin of Fig. D. Data are presented as the means ± SD of 3 independent experiments per treatment group. Significant differences of $p<0.01$ (*) are indicated.

Table1 : List of cell lines for cell-penetration assay

Cell line	Origin (histological type)
U87MG	Brain (glioblastoma)
U118MG	Brain (glioblastoma)
HeLa	Uterus (squamous cell carcinoma)
MSTO-211H	Lung (adenocarcinoma)
NCI-H226	Lung (adenocarcinoma)
A549	Lung (adenocarcinoma)
PANC-1	Pancreas (epithelioid carcinoma)
HepG2	Liver (hepatoblastoma)
Caco-2	Colon (adenocarcinoma)
HEK293	Non-neoplastic, embryonic kidney
Neuron	Brain (mouse hippocampal neuron)

A

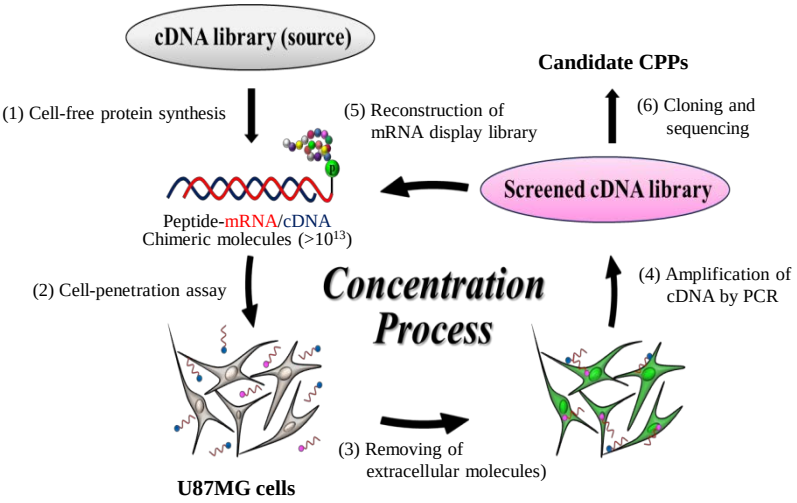

B

Peptide	Amino acid sequence	Length (a.a.)
Peptide 1	NTCTWLKYHS	10
Peptide 2	CASGQQGLLKLC	12
Peptide 3	YNNFAYSVFL	10
Peptide 4	ECYPKKGQDP	10
Peptide 5	RHVYHVLLSQ	10
peptide 6	HATKSQNINF	10
Peptide 7	YRDRFAFQPH	10
Peptide 8	IWRYSLASQQ	10
Peptide 9	YQKQAKIMCS	10
peptide 10	VQLRRRWC	8
R9	RRRRRRRRR	9

C

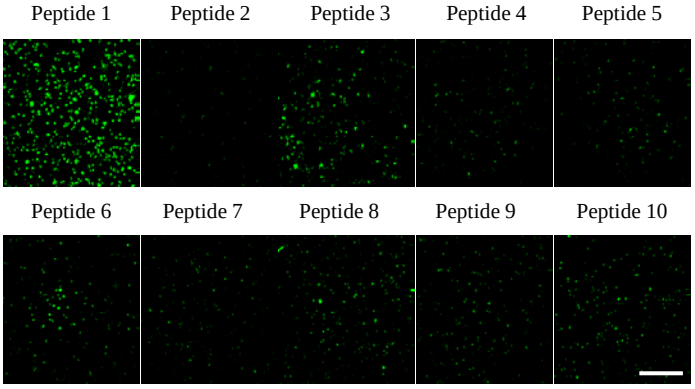

D

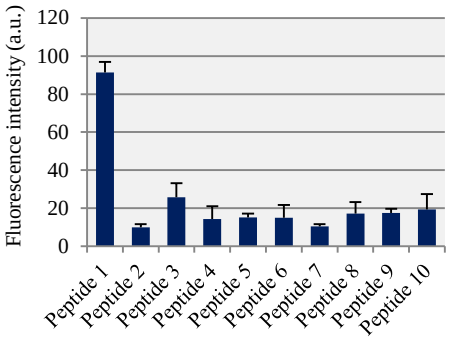

Figure 1

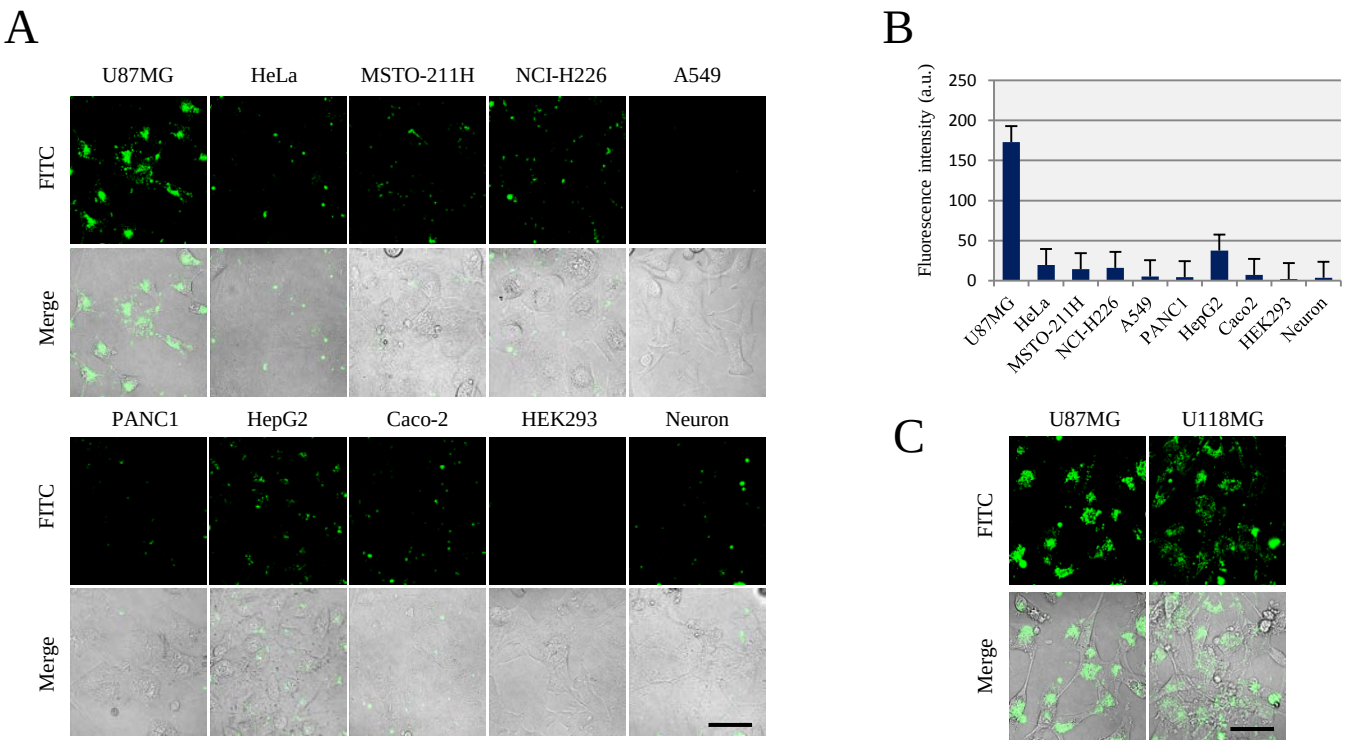
A
U87MG
HeLa
MSTO-211H
NCI-H226
A549
FITC
Merge
PANC1
HepG2
Caco-2
HEK293
Neuron
FITC
Merge
B
Fluorescence intensity (a.u.)
250
200
150
100
50
0
U87MG
HeLa
MSTO-211H
NCI-H226
A549
PANC1
HepG2
Caco2
HEK293
Neuron
C
U87MG
U118MG
FITC
Merge

Figure 2

Table2 : Amino acid sequence of the peptide1 variants

Peptide	Amino acid sequence	Length (a.a.)
Peptide 1	NTCTWLKYHS	10
Peptide 1-C3G	NTGTWLKYHS	10
Peptide 1-NΔ	TCTWLKYHS	9
Peptide 1-SΔ	NTCTWLKYH	9
Peptide 1-NSΔ	TCTWLKYH	8
Peptide 1-NTSΔ	CTWLKYH	7
Peptide 1-NTCSΔ	TWLKYH	6
Peptide 1-NTHSΔ	CTWLKY	6

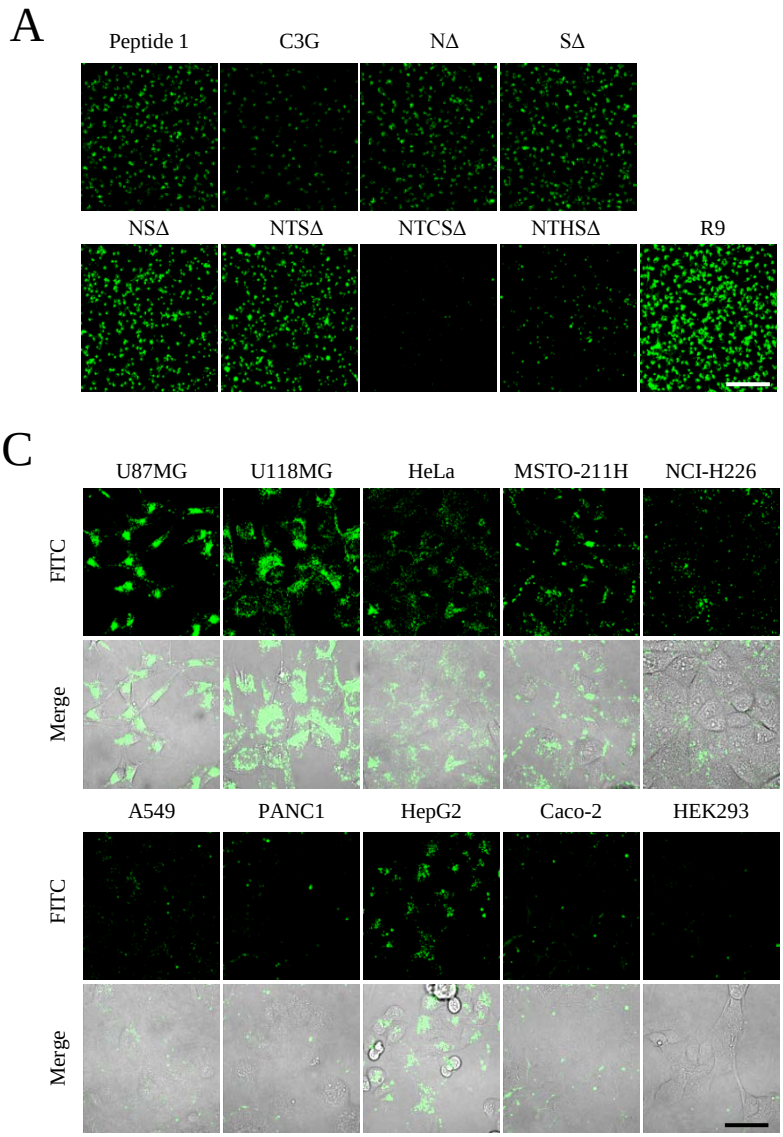
A
Peptide 1
C3G
NΔ
SΔ
NSΔ
NTSΔ
NTCSΔ
NTHSΔ
R9
B
Relative penetration efficiency (old)
2.5
2
1.5
1
0.5
0
Peptide1
C3G
NΔ
SΔ
NSΔ
NTSΔ
NTCSΔ
NTHSΔ
C
U87MG
U118MG
HeLa
MSTO-211H
NCI-H226
FITC
Merge
A549
PANC1
HepG2
Caco-2
HEK293
FITC
Merge
D
Fluorescence intensity (a.u.)
300
250
200
150
100
50
0
U87MG
U118MG
HeLa
MSTO-211H
NCI-H226
A549
PANC1
HepG2
Caco-2
HEK293

Figure 3

A

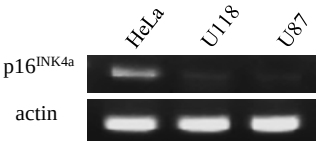

B

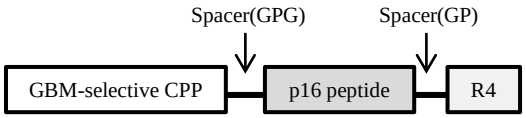

Peptide1NSΔ-p16 MIS
: TCTWLKYH-GPG-FLDTLVVLHR-GP-RRRR

Peptide1NSΔ-p16 V95E
: TCTWLKYH-GPG-FLDTLEVLHR-GP-RRRR

C

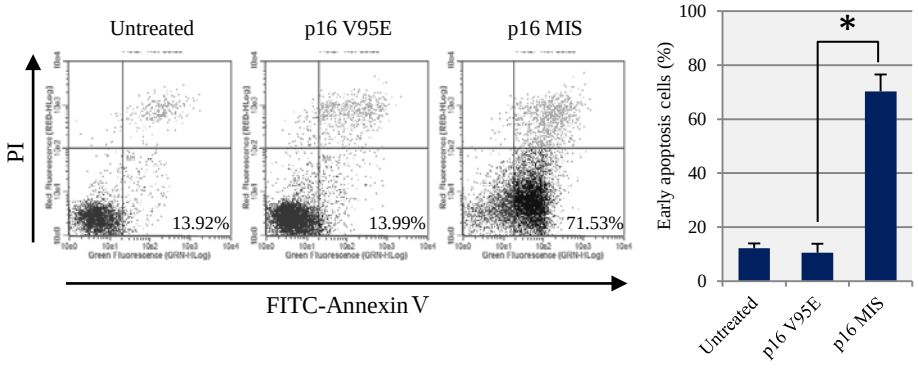

D

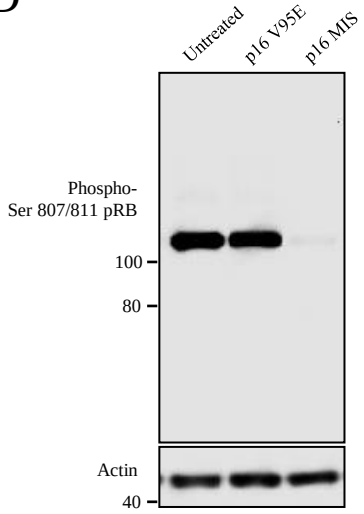

E

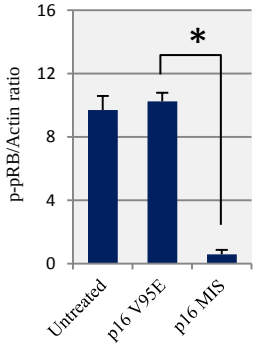

Figure 4